A COUPLED PERIDYNAMICS AND DEM-IB-CLBM METHOD FOR SAND EROSION PREDICTION IN A VISCOUS FLUID

Y. ZHANG[1], S. HAERI[2*], Y.H. ZHANG[2] AND G. PAN[1]

[1] Key Laboratory for Unmanned Underwater Vehicle,
School of Marine Science and Technology,
Northwestern Polytechnical University
Xi'an, Shaanxi 710072, China

[2] James Weir Fluid Laboratory, Department of Mechanical and Aerospace Engineering,
University of Strathclyde
UK, G1 1XJ

Key words: Erosion, Peridynamics, Fully Resolved Fluid-Particle interaction

Abstract. In this paper the peridynamics theory is integrated with a DEM-IB-CLBM (Discrete Element-Immersed Boundary-Cascaded Lattice Boltzmann Method) framework to enable fully-resolved simulations of sand erosion in viscous fluids. The crack and damage of the material walls are modelled with the peridynamics theory, the no-slip boundary condition is implemented on the surface of particles using an Immersed Boundary Method (IBM) and particle collisions are accurately resolved using a Discrete Element Method. The method is validated by comparing the trajectory of a particle colliding with a wall in a viscous fluid with the previous results provided in the literature. The impact of the generated craters due to the collisions on the vortex field and also the impact of collision angle on the material damage are investigated.

1 INTRODUCTION

The presence of solid particles (such as sand) in many flow instruments and pipelines, leads to major erosion problems such as degradation of pipelines and production equipment including pumps and valves. The impinging particles will cause excessive damage to the surface layer, which will also reduce the effectiveness of corrosion inhibitors resulting in material degradation. Meanwhile, corrosion will in return accelerate the erosion rate resulting in severe and repaid loss of surface metal (washout). The material defect may shorten the lifetime of pipelines and increase production risk. The lack of predictive design tools has resulted in overly conservative estimates of the life time of the equipment to avoid catastrophic failures.

The sand erosion problem is a complex phenomenon and involves the interplay of several parameters and physical phenomena including the flow pattern and geometry, fluid properties, particle size/shape distribution and particle/surface material characteristics

[1, 2]. Computational Fluid Dynamics (CFD) codes coupled with un-resolved particle tracking techniques (Eulerian-Lagrangian) and empirical erosion models have been employed [3, 4, 5, 6], to predict erosion rates in different geometries. In these studies, CFD techniques are used to provide a solution for the fluid flow field and particle trajectories. Based on calculated collision characteristics with the wall (such as collision velocity and frequency), the erosion rate is then estimated based on empirical models.

However, comprehensive reviews of particle erosion modelling techniques and the dynamics of the erosion process caused by the continuous particle impingement show the inadequacy of the erosion models [7, 8, 9]. The general consensus is that the available empirical models should be used with utmost care since they fail to include the effects of several important parameters. The available models are also subject to significant statistical inaccuracies since the model parameters are often calculated by fitting semi-empirical equations to scattered experimental data. Therefore, development of a framework to simulate sand erosion based on first principles is urgently required [7, 8, 9].

Several challenges are present for the development of a high-fidelity framework, these include estimation of material deformation and crack propagation, dealing with the deforming material surface immersed in the fluid and achieving a coupling between the material and flow field. In order to simultaneously consider these effects, naturally, a multi-physics framework is required: a numerical method that can solve the fluid flow field coupled with particle motion, particle impacts, material damage and the interactions among them. In this paper, the particle-wall collision in a viscous fluid is considered as a classical problem. The fluid, rigid particles and the variable material surface are solved with a recently developed coupled Discrete Element, Immersed Boundary, Cascaded Lattice Boltzmann Method (DEM-IB-CLBM). The framework has been fully validated and can accurately estimate the particle motion in the fluid. The DEM-IB-CLBM framework naturally couples with the Peridynamics (PD) theory [10] implemented using a particle based method.

In this paper, the PD theory is coupled with the DEM-IB-CLBM approach. This allows us to achieve a fully-coupled material and fluid solver. The impact of rigid particles will change the location and velocity of the material particles according to the PD theory. The material particles on the surface will also act as "Lagrangian" IBM forcing points to implement a no-slip boundary condition. The multi-physics PD-DEM-IB-CLBM framework is applied to obtain the dynamics of erosion for single particle-wall collision. The combined method can provide a detailed erosion process of the target material and predict erosion caused by multiple particle impingements. However, it should be noted that our emphasis here is on the development of a new numerical framework. The algorithm efficiency is not considered here and hence to manage the computational costs we completely remove the chipped surface material from the simulations. In future a threshold factor will be introduced to only remove chipped material of certain sizes, however, this requires further improvement to the algorithm to efficiently deal with the newly generated particles in the computational domain.

2 METHODOLOGY

2.1 Peridynamics theory

The PD equation of motion relates the time derivative of displacement of each PD particle, to the integral of an internal force field $\mathbf{f}(\eta, \xi)$ and an additional external force $\mathbf{F}_b$. The PD theory uses an integral to represent the relative displacement and force between neighbouring material points. Compared to the classical formulation based on partial derivatives, PD remains valid along discontinuities and hence directly captures any fracture or damage [10]. More details about the PD can be found elsewhere [10], however, here we briefly discuss the theory for completeness. The PD theory formulates the motion of material points by

$$\rho_m \ddot{\mathbf{u}}(\mathbf{x}, t) = \int_H \mathbf{f}(\eta, \xi) dV_{\mathbf{x}'} + \mathbf{F}_b(\mathbf{x}, t) \qquad \forall \mathbf{x} \in R, \tag{1}$$

where ρ_m is the density of material points, $\mathbf{u}$ is the displacement vector of the material point $\mathbf{x}$ at time t and $\mathbf{F}_b$ is a body force. The neighbourhood of the material point at $\mathbf{x}$ is represented by H, and it is determined by a parameter δ which is commonly referred to as a horizon (here, $\delta = 3.015 dx$). The internal force exerted on the material point $\mathbf{x}$ by all points $\mathbf{x}'$ within a neighbourhood of $\mathbf{x}$ is the integral of a force density $\mathbf{f}(\eta, \xi)$ over the volume $V_{\mathbf{x}'}$, where $\xi = \mathbf{x} - \mathbf{x}'$ is the relative position vector and $\eta = \mathbf{u} - \mathbf{u}'$ is the relative displacement vector.

A brittle material is considered in this paper using a Peridynamic bond-based prototype microelastic brittle (PMB) model [10]. In this model the force density is defined by

$$\mathbf{f}(\eta, \xi) = cs(\eta, \xi)k\mathbf{n}, \tag{2}$$
$$s(\eta, \xi) = \frac{||\eta + \xi|| - ||\xi||}{||\xi||}.$$

The constant c is related to the material property. If the stretch s exceeds its critical value s_0, the bond breaks irreversibly by setting k to zero, else $k = 1$. The unit vector $\mathbf{n}$ points from $\mathbf{x}$ to $\mathbf{x}'$. This allows material damage to be incorporated into the PD model. Local damage of a material point is defined as the ratio of the number of broken bonds to the total number of bonds. When the local damage is larger than a critical value s_c, the point is just excluded by cutting its connections to other material points and the point is permanently removed from the simulation. The critical value is set to 0.8 in this study [10]. The explicit integration of Eq. 1 allows a straightforward calculation of the displacement vector field $\mathbf{u}$. It requires a numerical stability condition, which leads to a critical time step δt_c^{pd} [11].

2.2 The DEM-IB-CLBM approach

The Cascaded Lattice Boltzmann Method (CLBM) accurately provides the flow field while the Immersed Boundary Method (IBM) implements the no-slip condition by adding a forcing term ($\mathbf{F}_{ibm}$) to Lagrangian points and distributing it onto the surrounding fluid nodes with a compact support [16, 18].
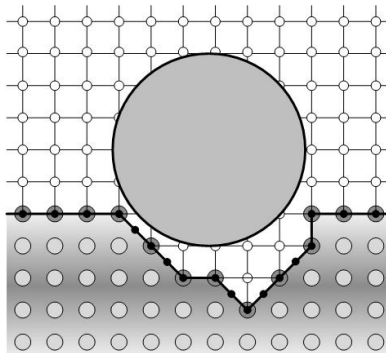
Figure 1: An illustration of the combined method. The LBM Lattices: ∘; The IBM points: •; The PD material points: ○; The exposed material points: ●.

In the DEM-IB-CLBM approach, the hydrodynamic force acting on the particle is directly calculated compared to unresolved methods where a model equation is required [17, 19]. The hydrodynamic force $\mathbf{F}_h$ on a particle is calculated by adding up $\mathbf{F}_{ibm}$ contributions of IB points and is used to calculate the particle trajectory in the fluid

$$\rho_p \frac{d\mathbf{U}(t)}{dt} = \mathbf{F}_h + \mathbf{F}_c + \mathbf{G}, \tag{3}$$

$$I_p \frac{d\mathbf{\Theta}(t)}{dt} = \mathbf{T}_h + \mathbf{T}_c. \tag{4}$$

In Eqs. (3) and (4), ρ_p is the density of the particle, $\mathbf{F}_c$ is the collision force, $\mathbf{G}$ is the gravity and $\mathbf{T}_h$ and $\mathbf{T}_c$ are collision and hydrodynamics torque correspondingly. $\mathbf{F}_c$ comprises the collision forces with other rigid particles $\mathbf{F}_c^{dem}$ (calculated using the DEM solver) and the collision with material points $\mathbf{F}_c^{pd}$. For the DEM stage of the solver, a spring-dashpot model is used to model collisions and a critical time step δt_c^{dem} is defined to perform the collision [20, 21].

2.3   The combined Peridynamics and DEM-IB-CLBM approach

Considering the fixed Eulerian mesh for the fluid domain, the size of Peridynamics material point is the same as lattice spacing dx of CLBM. Initially, the location of material points $\mathbf{x}$ coincide with lattice points, as shown in Figure 1.

The coupled algorithm is presented in Figure 2. Here, the IBM acts as an interface that connects the other three solvers together (DEM, PD, and CLBM) by calculating forces $\mathbf{F}_h^p, \mathbf{F}_h^{pd}$, and $\mathbf{F}_{ibm}$. The IB solver receives the information of flow field at the Lagrange points on the surfaces of particles and material. The presence of the PD points adds more complexity to the DEM and IBM solvers. The DEM solver calculates the impact forces $\mathbf{F}_r$ to the material points and $\mathbf{F}_c^{pd}$ to rigid particles. Then $\mathbf{F}_r$ is transferred to the PD solver through the exposed material points. The position of exposed PD points (and consequently the IB points) is then updated according to the PD solution.

The material with high Young's modules exhibit high-frequency oscillations when they are subjected to a sudden impact. To capture the oscillation, a high time-resolution is
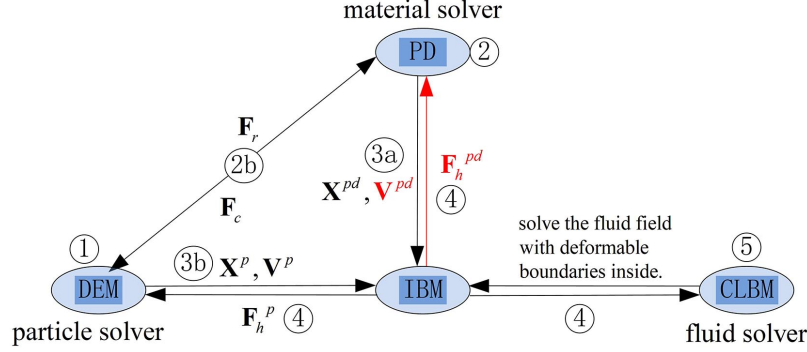
Figure 2: The structure of the combined method.

required otherwise this will result in numerical instability. The time step of the DEM-IB-CLBM approach should be small enough to capture the fluid phenomena accurately and resolve the collisions. By satisfying the fluid time step size restrictions the δt_c^{dem} (the time step size requirement of the DEM solver) is also satisfied. However, most brittle materials have a relatively high Young's module. If we choose a time step satisfying δt_c^{pd}, the computational costs will be huge and a further improvement is required. Therefore, a time step δt small enough to capture the fluid phenomena is employed as an overall critical time step. To fit the PD solver into the framework, a sub-iteration of the PD solver is used to compensate the time step gap between δt and δt_c^{pd}. The step-by-step algorithm can be summarised as follows

1. DEM deals with the contact between rigid particles;

2. Find the number of sub-iteration of the PD solver $\delta t / \delta t_c^{pd}$;

    (a) Compute the internal forces between material points according to Eq. 2;
    (b) Detect rigid particle-material point (exposed) collisions, add $\mathbf{F}_r / V$ to $\mathbf{F}_b$ (Eq. (1)), add $\mathbf{F}_r$ and $\mathbf{T}_r$ to the total force and torque of rigid particles;
    (c) Update the displacement of material points according to Eq. 1;

3. Update the location and the velocity of all Lagrangian points (IB points);

    (a) Transfer the location and velocity of exposed material points to the IB points.
    (b) Update the centres of rigid particles, locate IB points;

4. IBM enforces the no-slip boundaries immersed in a flow field; transfer the hydrodynamic forces to PD and DEM parts, get the refined velocity field for CLBM;

5. CLBM solves the flow field.

In addition, the effect of the hydrodynamic force on the flexible wall is ignored by setting $\mathbf{F}_h^{pd}$ to zero, since for a brittle material they are much smaller than the material's internal forces. The velocity $\mathbf{V}^{pd}$ is then computed as follow

$$\mathbf{V}^{pd,t} = (\mathbf{X}^{pd,t} - \mathbf{X}^{pd,t-\delta t})/\delta t. \tag{5}$$
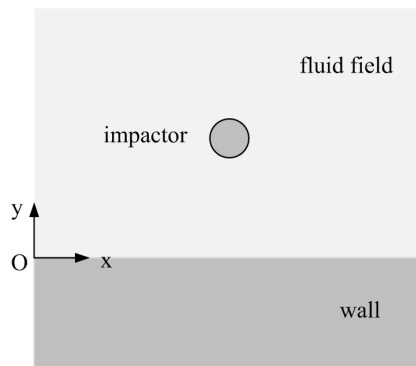
Figure 3: The geometry of the particle-wall collision in a viscous fluid.

3   VALIDATION

The combined method is validated considering the particle-wall collision problem. The geometry is shown in Figure 3. The gravitational constant is 9.81 m/s^2, the density and the dynamic viscosity of fluid are 1.0 g/cm^3 and 0.1 cm^2/s, respectively. A rectangular fluid domain of size $[10D, 8D]$ is used and the particle is positioned at $[5D, 2D]$. There are 50 lattices over the particle's diameter, $D = 50dx$. A zero-gradient boundary condition is applied to all the boundaries. The material plate is of size $[10D, 2D]$ and is positioned below the fluid domain.

Table 1: The physical properties of the surface and the particle.

Material Properties			
Length	L	m	0.03
Width	W	m	0.006
Young's module	E	Gpa	55
Poisson's ratio	ν	1	0.3333
Density	ρ_m	kg/m^3	2500
Critical stretch	s_0	1	0.01
Time step size	δt^{pd}	s	3.6×10^{-9}
Particle			
Diameter	D	m	0.003
Density	ρ_p	kg/m^3	7800

A restitution coefficient of $r_c = 0.97$ is required to compare the particle rebound velocity to the literature [13]. However, the restitution coefficient r_c and the contact duration T_c also depend on the boundary conditions of the plate if a PD solver is used. The physical parameters [14] are displayed in Table 1 and two tests were performed with free and fixed boundary conditions for the bottom of the solid wall, where the lateral boundaries are fixed and the upper boundary free. The impact velocity in the absence of any fluid is
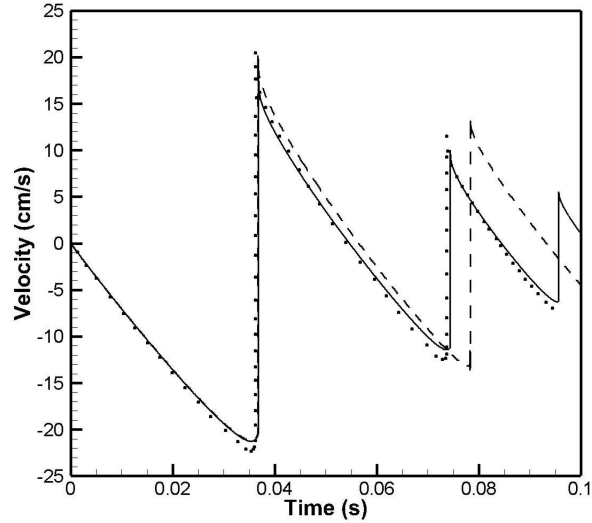
Figure 4: The vertical velocity of the particle moving in fluid varies with time. Results from Ref. [13]: black dots; DEM: solid line; PD: dashed line.
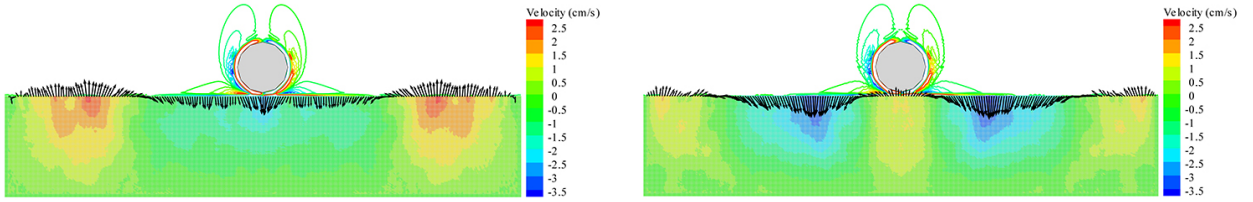

Figure 5: The vortex fields of fluid, the vertical velocity fields of the material plate, and the velocity vectors of the IB points on the surface of the material plate at different moments of the first rebound.

$V_{imp} = 21$ cm/s.

For a free bottom boundary, the calculated r_c is 0.44, far from 0.97. However, for a fixed bottom boundary, r_c is 0.97. The rebound finishes in a short contact duration of $T_c = 7$ μs. The number of time steps over T_c is set as $N_{cd} = 260$, which means $dt = T_c/N_{cd}$. Figure 4 shows that the results of DEM agree well with the literature [13] for a rigid plate. For a material plate which allows for deformation, the rigid particle rebounds with a higher velocity which we believe is related to the deformation of the material plate and transfer of energy to the particle.

The vortex field of fluid and the velocity field of the material are shown in Figure 5. It shows the reaction of material to the particle impact in an ambient fluid and the importance of employing realistic material models in the investigation of particle-wall collision in a viscous fluid.

7

4   EROSION INDUCED BY PARTICLE–WALL COLLISION

In this section, the effectiveness of the new coupled framework to predict erosion is demonstrated by considering the damage caused by collision of a single particle with a wall.

Figure 3 shows the setup of the test problem in this section. The material properties are similar to those used in the previous section. Several fluid forces such as drag and added-mass effects should be considered particularly for fluid with higher viscosities and the current method is capable to directly include these effects without any further models. The particle is released normally at a distance $1.5D$ away from the material surface. A liquid- and a gas-like medium are chosen. The density ρ and the viscosity ν of the liquid and the gas are 0.935 g/cm^3 and 0.1 cm^2/s, 0.001 g/cm^3 and 0.15 cm^2/s, respectively.

The particle is released with a velocity of 30 m/s in both media. For the liquid-like fluid, initially the particle velocity drops sharply and then further decrease is observed until the impact with a velocity near 21 m/s. On the other hand, there is little velocity reduction for the particle in a gas-like medium. When the particle hits the material plate, the due to material damage, penetration into the material plate occurs. Therefore, the restitution coefficients come close to zero. However, it should be noted that our initial implementation removes all PD points that are separated from the main body (chipped material). A more realistic situation could be simulated by removing the chipped material only if they are smaller than a threshold value. However, this will substantially increase the computational costs since the newly generated particles should be resolved in the computational domain, therefore the a grid adaptation algorithm is required.

The flow field during the particle impact is quite different due to the appearance of craters as displayed in Figure 6. Two symmetric vortexes are generated above the particle while it settles. On the rigid plate, the two main vortexes move downward along the particle's surface profile, while several small vortices form below the particle. In contrast, the growth of a crater strengthens the two symmetrical vortexes below the particle due to ejection of fluid after each collision. For particles with a higher impact velocity in the gas, the depth and size of the crater are larger and the vortexes below the particle are stronger. These symmetrical vortexes move away from the crater along the material surface.

The craters in Figure 6 formed by the normal impact of the particle in the gas resembles the well-known cone cracks and the shape is very similar to the experimental results [2, 15]. The experiments of Knight et. al [15] present the crack distribution resulting from the impact of a 1 mm steel particle with a velocity of 26 m/s, where no radial and lateral cracks appear. The present Peridynamics model does not include the ductility and the historical effects of material however more sophisticated and realistic models could be implemented to include these phenomena.

Brittle materials usually suffer from maximum damage during a normal collision [9, 22]. Here the particle is released in a gas and a liquid, at (10°, 30°, 50°, 70°) and the same velocity of 30 m/s from a constant distance $1.5D$ to the impact point. The material damage is calculated by adding up the number of broken bonds to the total number of
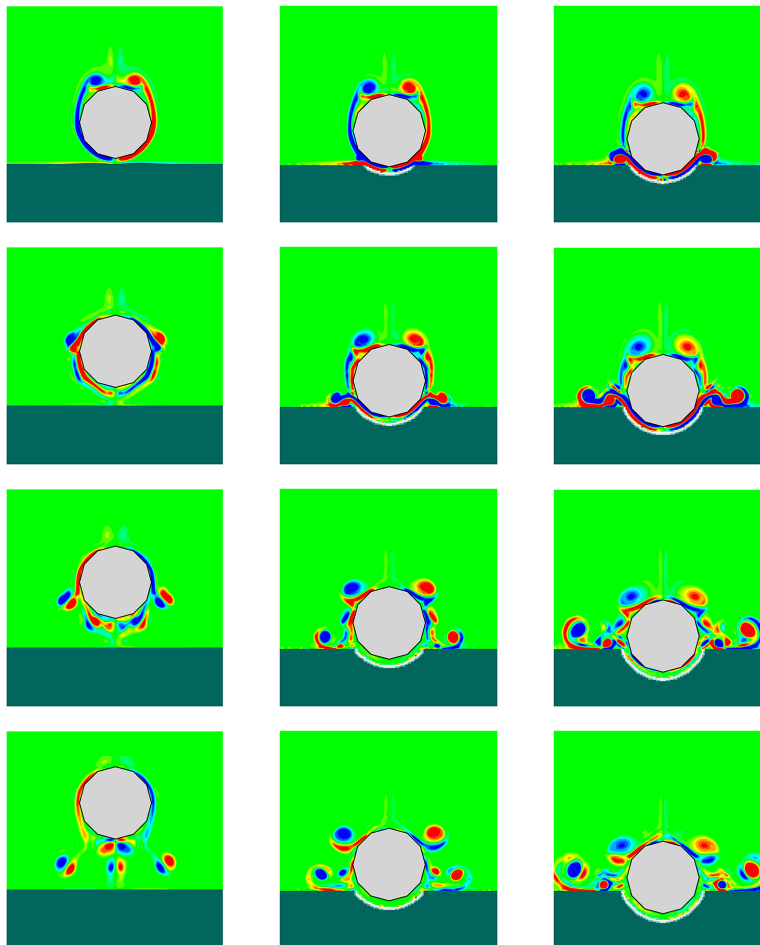
Figure 6: The vortex field at different instants of particle's normal impact. The particle is released with initial velocity 30 m/s, liquid with a rigid plate (left column), liquid with a PD plate (middle column), gas with a PD plate (right column).

bonds as explained earlier and the results are presented in Figure 7. Despite the different maximum damage values in the fluid and gas, similar increase in the damage is observed for both cases. Interestingly, the curve shows a maximum gradient between $\approx 15° - -50°$ and reaches a plateau after that.

5   CONCLUSIONS

We present a novel algorithm by integrating the peridynamics theory into our DEM-IB-CLBM framework to fully resolve the erosion induced by solid particle impacts. The fully resolved particle-fluid coupling (DEM-IB-CLBM approach) provides accurate trajectories of the particles and their rotational and translational kinetic energies just before the impact. The PD theory then directly predicts the material damage due to the impact. The coupled framework provides invaluable information regarding the erosion mechanisms, which is not available through any other simulation technique. Improvements are
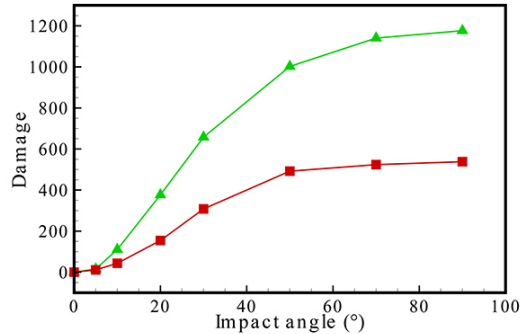
Figure 7: The damage as a function of impact angle. The initial velocity is set to 30 m/s.

necessary however, to enable quantitative comparison with experimental results. These improvement include development of more realistic PD material models for the current framework and also improvements to the simulation algorithm to consider large chipped material into the solution process.

ACKNOWLEDGMENT

REFERENCES

[1] Hutchings, I.M. A model for the erosion of metals by spherical particles at normal incidence. *Wear* (1981) **70**:269–281.

[2] Walley, S.M. and Field, J.E. The contribution of the Cavendish laboratory to the understanding of solid particle erosion mechanisms. *Wear* (2005) **258**:552–566.

[3] Aponte, R.D. Teran, L.A. Ladino, J.A. Larrahondo, F. Coronado, J.J. and Rodríguez, S.A. Computational study of the particle size effect on a jet erosion wear device. *Wear* (2017) **374**:97–103.

[4] Vieira, R.E. Mansouri, A. McLaury, B.S. and Shirazi S.A. Experimental and computational study of erosion in elbows due to sand particles in air flow. *Powder Technology* (2016) **288**:339–353.

[5] Liu, H.X. Zhou, Z.W. and Liu, M.Y. A probability model of predicting the sand erosion profile in elbows for gas flow. *Wear* (2015) **342**:377–390.

[6] Lee, B.E. Tu, J.Y. and Fletcher, C.A.J. On numerical modeling of particle–wall impaction in relation to erosion prediction: Eulerian versus Lagrangian method. *Wear* (2002) **252**:179–188.

[7] Parsi, M. Najmi, K. Najafifard, F. Hassani, S. McLaury, B.S. and Shirazi, S.A. A comprehensive review of solid particle erosion modeling for oil and gas wells and pipelines applications. *Journal of Natural Gas Science and Engineering* (2014) **21**:850–873.

[8] Ben-Ami, Y. Uzi, A. and Levy, A. Modelling the particles impingement angle to produce maximum erosion. *Powder Technology* (2016) **301**:1032–1043.

[9] Zheng, C. Liu, Y.H. Chen, C. Qin, J. Ji, R.J. and Cai, B.P. Numerical study of impact erosion of multiple solid particle. *Applied Surface Science* (2017) **423**:176–184.

[10] Silling, S.A. and Askari, E. Peridynamic modeling of impact damage. *ASME/JSME 2004 Pressure Vessels and Piping Conference* (2004) :197–205.

[11] Madenci, E. and Oterkus, E. *Peridynamic theory and its applications*. Springer, 1st Edition, 2014.

[12] Luding, S. Introduction to discrete element methods: basic of contact force models and how to perform the micro-macro transition to continuum theory. *European Journal of Environmental and Civil Engineering* (2008) **12**:785–826.

[13] Ardekani, A.M. and Rangel, R.H. Numerical investigation of particle–particle and particle–wall collisions in a viscous fluid. *Journal of fluid mechanics* (2008) **596**:437–466.

[14] Gondret, P. Lance, M. and Petit, L. Bouncing motion of spherical particles in fluids. *Physics of fluids* (2002) **14**:643–652.

[15] Knight, C.G. Swain, M.V. and Chaudhri, M.M. Impact of small steel spheres on glass surfaces. *Journal of Materials Science* (1977) **12**:1573–1586.

[16] Haeri, S. and Shrimpton, J.S. On the application of immersed boundary, fictitious domain and body-conformal mesh methods to many particle multiphase flows *International Journal of Multiphase Flow* (2012) **40**:38–55.

[17] Haeri, S. and Shrimpton, J.S. A mesoscopic description of polydispersed particle laden turbulent flows *Progress in Energy and Combustion Science* (2011) **37**:716–740.

[18] Haeri, S. and Shrimpton, J.S. A new implicit fictitious domain method for the simulation of flow in complex geometries with heat transfer *Journal of Computational Physics* (2013) **237**:21-45.

[19] Shrimpton, J.S. Haeri S. and Scott, S.J. Statistical Treatment of Turbulent Polydisperse Particle Systems *Springer-Verlag* (2011).

[20] Haeri, S. Wang, Y and Ghita, O. and Sun, J. Discrete element simulation and experimental study of powder spreading process in additive manufacturing *Powder Technology* (2017) **306**:4554.

[21] Haeri, S. Optimisation of blade type spreaders for powder bed preparation in Additive Manufacturing using DEM simulations *Powder Technology* (2017) **321**:94-104.

[22] Bitter, J. A study of erosion phenomena, part 2. *Wear* (1963) **6**:169–190.